4th Imeko TC19 Symposium on Environmental Instrumentation and Measurements
Protecting Environment, Climate Changes and Pollution Control
June 3-4, 2013, Lecce, Italy

THE USE OF A MULTIWAVELENGTH LIDAR TO DETECT AEROSOL LAYERS IN THE ATMOSPHERE

Ferdinando De Tomasi *and Maria Rita Perrone*

Dipartimento di Matematica e Fisica “Ennio De Giorgi”, Università del Salento, Lecce,Italy.
Consorzio Nazionale Interuniversitario per le Scienze della Materia (CNISM)
Ferdinando.DeTomasi@le.infn.it

Abstract: The peculiarity of lidar systems is to provide vertical profiles of aerosol extinction and backscattering coefficients, which allow getting information on aerosol optical properties and their dependence on altitude. We analyze in this paper a case study in which lidar signals have allowed detecting different atmospheric aerosol layers from the boundary layer up to the stratosphere. Results on the dependence of aerosol optical properties on altitude will also be presented.

Keywords: Lidar, aerosol, stratosphere, volcanic eruption .

1. INTRODUCTION

Many efforts have been dedicated in the last two decades in the development of devices for the remote sensing of atmospheric aerosol. A global sun photometer network, AERONET, has been established and different spectrometers sensitive to aerosol properties are onboard of satellites. However, these instruments have no profiling capabilities, which is instead important to investigate aerosol effects on climate. Atmospheric aerosols are mainly located in the Planetary Boundary Layer (PBL). However, they can also be found above the PBL, mainly because of long range transport, and the contribution of such high aerosol layers can be not negligible in aerosol-climate studies. The knowledge of the aerosol load vertical profile is important because of the direct and indirect aerosol effects on climate. In addition, the aerosol load within the PBL is the result of a balance between the local aerosol production and the long-range transport of aerosol. Understanding aerosol transport needs models to be initialized and fed with real data. The main tool for the aerosol profiling is the LIDAR (Light Detection And Ranging) [1]. A lidar system is composed by a pulsed laser and a collection and detection system that detects the backscattered laser radiation, both from atmospheric molecules and aerosol. The aerosol vertical distribution is obtained by the time resolved detection of the backscattered radiation.

In this paper we show a case study in which different kind of aerosols are observed from the PBL up to the stratosphere by a multiwavelength lidar.. Aerosol backscattered signals are spectral dependent, so that measurements at different wavelengths can help identifying aerosol of different types.

2. Elements of lidar theory

A lidar signal is determined by the backscattered radiation of a laser pulse; its dependence on altitude z and on the atmospheric components can be written as:

$$P(z) = C\beta(z)T(z)^2 \qquad (1)$$

where $P(z)$ is the so called “range-corrected” signal, i.e. the backscattered signal multiplied by z^2 . C is a calibration constant (whose value is not usually needed) , β is the total backscattering coefficient and T is the total transmission coefficient. Both these quantities are due to both aerosol and a molecular contributions (we suppose to operate at wavelengths where it is possible to neglect absorption by molecules):

$$\beta = \beta_{aer} + \beta_{mol} \qquad (2a)$$

$$T = T_{aer}T_{mol} \qquad (2b)$$

The transmission coefficient is determined by the total atmospheric extinction α:

$$T = \exp(-\int_0^z \alpha(z')dz') \qquad (3)$$

It is assumed that the molecular part is known with a sufficient approximation, by radiosoundings, atmospheric models, or a combination of them. Aerosol backscattering and transmission coefficients are independent quantities so that Eq.1 contains two unknowns. This is resolved using the lidar signal due to inelastic (Raman) scattering, and in this case Eq.1 transforms in a new equation where the aerosol backscattering coefficient is no more present. In cases in which the Raman signal is not available, a relation between the backscattering and extinction coefficient is assumed: in most cases this is a simple linear relationship so that it can be written

$$S = \alpha_{aer} / \beta_{aer} \quad (4)$$

The S parameter is known as "lidar ratio" and it is a characteristic of an aerosol population.

In a multi-wavelength lidar, signals corresponding to different laser wavelengths (λ) are collected, so that the spectral dependence of backscattering and extinction can be estimated. A useful parameter is the Angstrom coefficient

$$Å_{1\_2} = -\frac{1}{\ln(\frac{\lambda_1}{\lambda_2})} \ln(\frac{\alpha_{aer}(\lambda_1)}{\alpha_{aer}(\lambda_2)}) \quad (5)$$

which is close to zero when the size of particles is large compared to the wavelengths and increase when the particle size decreases (in the limit of very small particles, which is the case of molecular scattering, the Angstrom coefficient approaches the value 4) .

Laser light is usually polarized so that the depolarization of the backscatter coefficient contains information about the symmetry of the scatterers. Spherical particles conserve the polarization of the incident laser light. The presence of non-spherical particles results in a non zero polarization in the direction perpendicular to the laser polarization. If a polarization sensitive detector is used, Eq.1 is then split into two separated equations, so that the quantity

$$\delta = \frac{P_\perp}{P_\parallel} = \frac{\beta_\perp}{\beta_\parallel} \quad (6)$$

can be obtained by separate measurements of the polarization components of the backscattered light.

3. THE EXPERIMENTAL APPARATUS

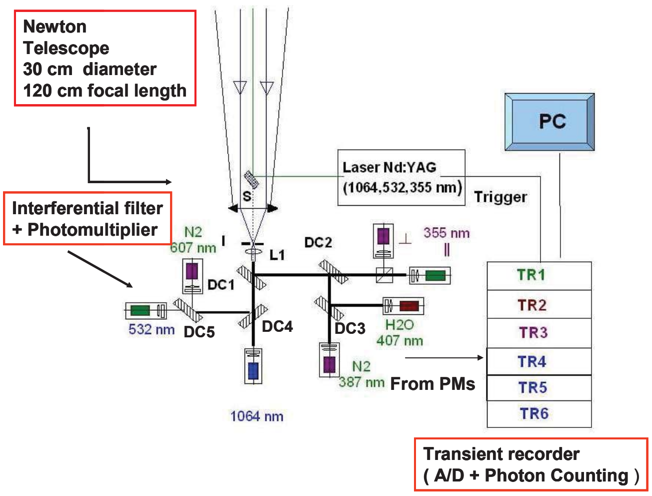

Figure 1. Sketch of the experimental apparatus. Legend: S: backscattered light from the atmosphere. I : Iris. L1 : collimation lens. DCs: dichroic mirrors.

The lidar UniLe is operating at the Mathematical and Physics Department of Università del Salento since 1999 [2]. It is part of the European lidar network EARLINET since its foundation, in 2000. The experimental apparatus is composed by a Nd:Yag laser operating at its fundamental wavelength, 1064 nm, and the second and third harmonic at 532 and 355 nm, respectively. Laser pulses are about 10 ns long. The maximum energy per pulse is 1000 mJ, 150 mJ and 300 mJ, at 1064, 532, and 355 nm, respectively. The spatially separated laser beams are recomposed by a set of dichroic mirrors and sent vertically in the axis of a f/4 Newton telescope. The backscattered radiation is collected by the primary mirror of the telescope and collimated by a plano-convex lens. The collimated beam is then sent into a polychromator where a selection of the wavelengths is operated by a set of dichroic mirrors and interferential filters. Three different sections corresponding to the three laser wavelengths are identified. First, the UV section detects the elastic scattering from aerosol and atmospheric molecules and the Raman scattering from N_2 and H_2O. Furthermore, the elastic scattering is split by a non polarising cube: the transmitted beam is detected, and the reflected beam is filtered by a plate polarizer to detect only the cross-polarized component. Thus, in the UV section, the system can measure the volume depolarization of the atmosphere at 355 nm, the backscattering coefficient, the extinction coefficient at 355 nm exploiting the Raman scattering from N_2, and the water vapour mixing ratio.

The green section detects the elastic scattering from the laser radiation at 532 nm and its inelastic component at 607 nm, from N_2, so that backscattering and extinction at these wavelengths can be retrieved. The infrared part detect simply the elastic backscattered signal at 1064 nm, being the Raman scattering at 1064 nm too small to be detected in normal conditions.

The 1064 signal is detected by an avalanche photodiode; all the other signals are detected by photomultipliers. Finally, the signals are sent to transient recorders that have both a 12 bit A/D conversion and a photon counting (PC) capability. In this way the full dynamic range of the signals can be covered gluing the A/D signals from low altitudes to the PC signals from higher altitudes in a range in which the signals are above the noise threshold and below the saturation level, respectively. The H_2O and the 1064 signals are respectively detected by single PC and A/D transient recorder (the H_2O Raman signal is usually low enough to avoid saturation and the photodiode used to detect 1064 does not detect single photons). Usually the transient recorders integrate over 2000 laser shots that correspond to about 60 s.

4. DISCUSSION OF LIDAR SIGNALS

The lidar is located in the suburb of Lecce, in a rural environment (40.33 N, 18.11 E). Figure 2 shows a color map (logarithmic) of the range corrected elastic signal at 532 nm acquired on July 4, 2011, between 18:30 and 19:30 UTC. These images are useful for a quick-look of the lidar signals and to highlight the main features of the atmospheric backscattered radiation. Also, such images are useful to identify temporal intervals in which lidar signals look homogeneous, so that they can be temporally averaged to improve the S/N ratio.

It is possible to deduce from this quick look image (Figure 2): 1) a low altitude layer, possibly due to a local PBL and a residual layer up to 2500 m. 2) a medium altitude layer from 2500 to 5000 m 3) an high altitude layer at stratospheric altitudes (larger than 15000 m). At the beginning and at the end of the acquisition a strong backscattered signal can be observed at about 10000 m from the ground level. This is typically a signature of cirrus clouds, as confirmed by the high volume depolarization ratio (not shown here).

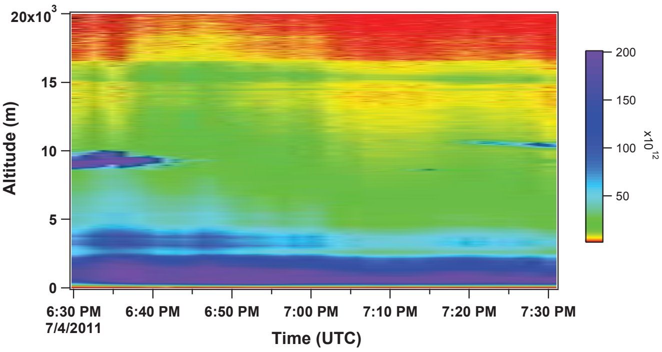

Figure 2. Logarithmic color map (arbitrary units) of the range-corrected signal at the 532 nm laser wavelength. Different features can be observed: two separate layers at altitude lower than 5000 m, cirrus clouds at about 10000 m, and a stratospheric aerosol layer above 15000 m from the ground level.

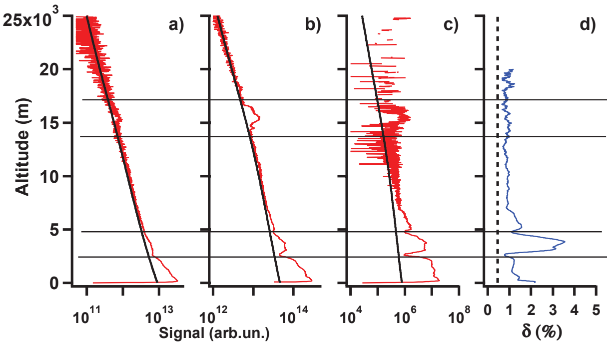

Figure 3. a-c) Averaged range-corrected lidar signals (logarithmitic scale) at a) 355, b) 532, and c) 1064 nm corresponding to cloud-free time intervals of Fig. 2. Black line, profiles represent the signal from a pure molecular atmosphere calculated by radiosoundings and a model (MSIS of NASA). d) Volume depolarization ratio at 355 nm. The dashed line is the value of the volume depolarization ratio from the aerosol free atmosphere. The black horizontal lines are a guide for the eye evidencing the layers in the atmosphere.

If we average the signals in the intervals corresponding to the absence of clouds, we obtain the elastic signals shown in Fig.3, where the aerosol layers are evidenced. The depolarization measurements are also shown in the figure. On the basis of the signals and the depolarization measurements, we can identify three main layers: a low-depolarizing layer at low altitudes, an high-depolarizing layer in the middle troposphere, and another low-depolarizing layer in the high troposphere.

Furthermore, a peak in the signals around 17000 m is displayed in each of the elastic signals, indicating the presence of stratospheric aerosol. In the figure, simulated signals corresponding to an aerosol free atmosphere are also shown. These simulated signals are necessary to identify ranges of altitudes that can be considered aerosol-free for calibration purposes. Also, a lidar signal that reduces to a pure molecular signal at high altitude is a proof that the system is working properly.

A first quantitative analysis of the lidar signals allows calculating the aerosol backscattering coefficient. This is done by standard methods [3], using a constant lidar ratio S=50. At 355 and 532 nm the calibration is made by a fit of the lidar signal at the molecular signal in the interval 25000-30000 m. At 1064 nm, it is not possible to apply this technique because of the high altitude of the aerosol free region and not enough S/N ratio at this altitude, thus a method relying on the cirrus backscattering signal has been used [3].

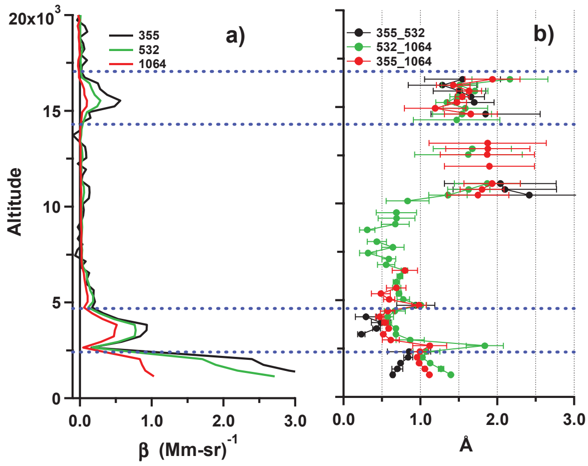

Figure 4. Vertical profiles of a) the aerosol backscattering coefficient at the three laser wavelengths and b) of the Angstrom coefficient for the different wavelengths pairs. Error bars represent the statistical error. Blue horizontal lines are a guide for the eye evidencing the layer of the atmosphere.

From aerosol backscattering coefficients it is possible to estimate extinction coefficients and then, to calculate the Angstrom coefficient. Figure 4 shows the aerosol backscattering coefficient at the three laser wavelengths and the Angstrom coefficient for different wavelengths pairs. Only data points that satisfy the following conditions are reported: if the value is larger than 0.1, the relative error must be minor than 0.5; if the value is less than 0.1, the absolute error must be lower than 0.3. Larger errors correspond obviously to region in which the backscattering coefficient is low. We can see from Fig. 4b that the Angstrom coefficient is different for different aerosol layers: the lower layer has an average Å =1, the second is instead significantly much lower (0.5). In the stratosphere, above 10000 m from the ground, the Angstrom coefficient becomes higher, around 1.5-2. In the layer corresponding to the aerosol stratospheric peak, it is possible to see that the statistical error reduces (because of the increased backscattered signal) and Å sets to a value of 1.5.

5. ORIGIN OF AEROSOL

From the above discussion, it is possible to conclude that two main tropospheric layers and one stratospheric layer are present. To assess the origin of these air masses, all available information should be used. Usually, dust particles have high depolarization and a low Angstrom coefficient, so that it is highly probable that the second layer between 2 and 5 km is composed by dust. The lowermost layer has a lower depolarization and an higher angstrom coefficient so that it seems decoupled from the higher one. One way to check this fact is to use air mass backtrajectory. In Fig.5a backtrajectories starting from Lecce and extending to 10 days are shown, for different arrival altitudes. It is possible to see that the lower altitude particles are down-lofted from higher altitudes. These air masses could be loaded with aerosol produced in forest fires in North-America.

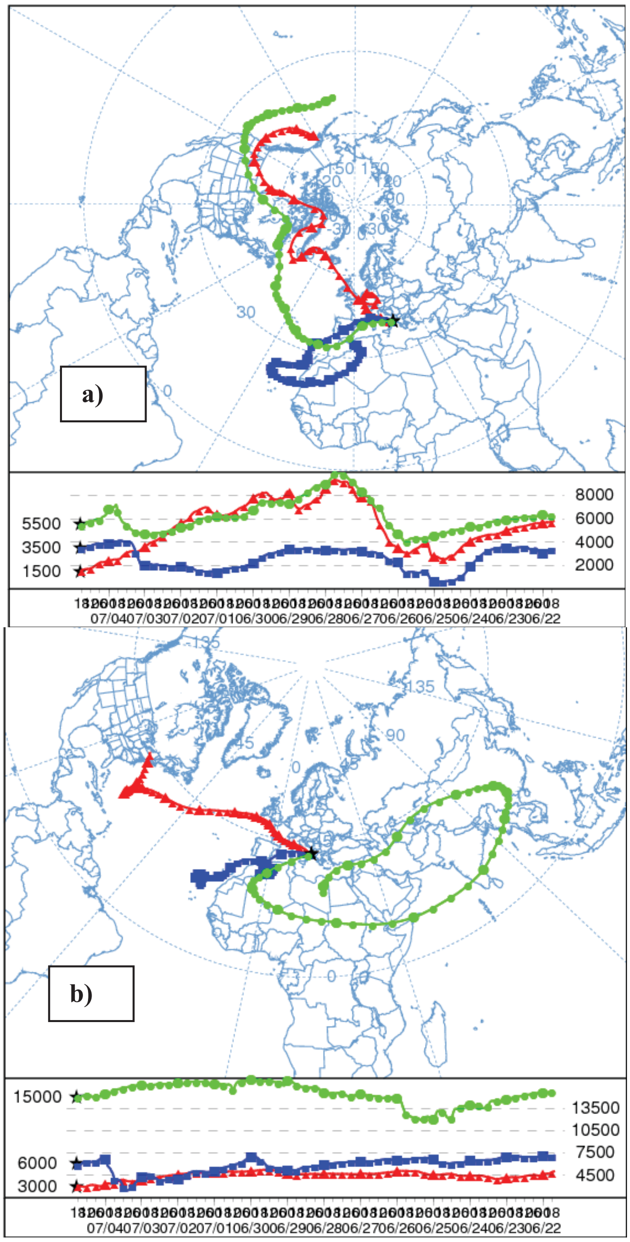

Figure 5. 12–days Backtrajectories plots obtained by the HYSPLIT model for the lidar site for July 4, 2011, 19 UTC, for different altitudes.

Trajectories corresponding to the altitudes of the second layer originates instead from Sahara region, however they are not directly transported through the Mediterranean but instead they travel along Atlantic European regions and then they arrives over the monitoring site. It is interesting to note that also at higher altitudes, outside the second layer, where the depolarization is lower but higher than the molecular values, trajectories appear to arrive from Sahara after long range transport (Fig. 5b).

Finally, the stratospheric layer must be discussed. This layer is characterized by a very low volume depolarization and an higher Angstrom coefficient, which indicates small, nearly spherical particles. Actually, stratospheric aerosol are usually produced by volcanic eruptions, that emits SO_2 that is converted to H_2SO_4 that can origin sulphates particles. In this period, actually, an eruption has been reported for the Nabro volcano in Eritrea. The eruption has been active between June and July 2011. Stratospheric aerosol have been observed in many stations in the world during this period, and also from the satellite lidar CALIPSO, so that it is very like that the observed peak is due to a volcanic plume [4]. The backtrajectories plots in Fig. 5b show that the observed air masses in the stratosphere crossed the Nabro region in the activity days.

6. CONCLUSION

We have shown in this paper how a multi-wavelength lidar can be used to discriminate between different aerosol layers measuring the particle depolarization ratio and the Angstrom coefficient. These techniques have been applied to a case study in which boundary layer, desert dust, and stratospheric aerosol were observed.

7. ACKNOWLEDGEMENTS

This work has been partially supported by the ACTRIS Research Infrastructure Project supported by the European Union Seventh Framework Programme (FP7/2007-2013) under grant agreement n. 262254.

8. REFERENCES

[1] C. Weitkamp (ed.), “Lidar. Range resolved remote sensing of the atmosphere”, Springer Series in Optical Sciences, vol 102, 2005.

[2] F. De Tomasi and M.R. Perrone, “Lidar measurements of tropospheric water vapour and aerosol profiles over southeastern Italy”, Journal of Geophysical Research-Atmospheres 108, 10.1029/2002jd002781, 2003.

[3] F. Navas-Guzman et al, “On the use of cirrus clouds for ground-based elastic lidar calibration” , Opt. Pura Apl., 44, pp 49-53, 2011.

[4] P. Sawamura et al, “Stratospheric AOD after the 2011 eruption of nabro volcano measured by lidars over the Northern Hemisphere” Environmental Research Letters , vol. 7, 034013 (9 pp) , 2012.